

## Article

# Characterization of Native and Human Serum Albumin-Bound Lysophosphatidic Acid Species and Their Effect on the Viability of Mesenchymal Stem Cells In Vitro

Aliz Majer <sup>1,2,\*</sup>, Julianna Pesthy <sup>1</sup>, Balázs Besztercei <sup>1</sup>, Adél Hinsenkamp <sup>1</sup>, László Smeller <sup>3</sup> , Zsombor Lacza <sup>2,4</sup>, Zoltán Benyó <sup>1</sup> , Éva Ruisanchez <sup>1</sup> and István Hornyák <sup>1,2</sup> 

<sup>1</sup> Institute of Translational Medicine, Semmelweis University, 1094 Budapest, Hungary

<sup>2</sup> Orthosera Medical Zrt., 1123 Budapest, Hungary

<sup>3</sup> Department of Biophysics and Radiation Biology, Semmelweis University, 1094 Budapest, Hungary

<sup>4</sup> Institute for Sports and Health Sciences, University of Physical Education, 1123 Budapest, Hungary

\* Correspondence: majer.aliz@med.semmelweis-univ.hu

**Abstract:** Scaffolds can provide a healthy environment for cell attachment, differentiation, proliferation, and migration in vitro and in vivo. Lysophosphatidic acid (LPA) is a naturally occurring bioactive phospholipid that is present in the serum mainly bound to albumin. The present study aims to investigate the biocompatibility of LPA. It also aims to determine the effect of different LPA species on the proliferation and migration of human bone marrow-derived mesenchymal stem cells (hBM-dMSCs) for LPA and human serum albumin (HSA) containing bone scaffold development. The HSA-LPA complex formation was assessed using Fourier-transform infrared (FTIR) spectroscopy. The effect of 18:1, 18:2, or 16:0 LPA alone, or in combination with 4% HSA, on cell viability and proliferation was determined by XTT. The cell migration was examined in a wound healing assay. The changes in the FTIR spectra of LPA-HSA compositions, compared with HSA alone, indicate the complex formation between the components. Our study showed that 18:1, 18:2, and 16:0 LPA species had no cytotoxic effects up to 10  $\mu$ M concentration. The different LPA species increased the proliferation of hBM-dMSCs in a dose-dependent manner when administered in the presence of HSA, without an effect on the migration of this cell type. These findings make the in vivo application of LPA-HSA complex promising for bone regeneration.

**Keywords:** lysophosphatidic acid; albumin; mesenchymal stem cells; scaffold; FTIR; viability; migration



**Citation:** Majer, A.; Pesthy, J.; Besztercei, B.; Hinsenkamp, A.; Smeller, L.; Lacza, Z.; Benyó, Z.; Ruisanchez, É.; Hornyák, I. Characterization of Native and Human Serum Albumin-Bound Lysophosphatidic Acid Species and Their Effect on the Viability of Mesenchymal Stem Cells In Vitro. *Appl. Sci.* **2022**, *12*, 8183. <https://doi.org/10.3390/app12168183>

Academic Editors: Eva Martins and Artur Turek

Received: 18 July 2022

Accepted: 14 August 2022

Published: 16 August 2022

**Publisher's Note:** MDPI stays neutral with regard to jurisdictional claims in published maps and institutional affiliations.



**Copyright:** © 2022 by the authors. Licensee MDPI, Basel, Switzerland. This article is an open access article distributed under the terms and conditions of the Creative Commons Attribution (CC BY) license (<https://creativecommons.org/licenses/by/4.0/>).

## 1. Introduction

In the field of tissue engineering and regenerative medicine (TERM), there are two main approaches toward clinical application in human subjects. The most convenient approach is developing a service that can be used for regenerative interventions, such as surgery-related techniques, cell-based therapies, gene therapy, and immunomodulation. These are usually in-house developed techniques that can enable, e.g., a clinician to implant a bone substitute for dental or weight-bearing surgeries. These techniques often require unique knowledge that is limited to persons skilled in this art. The other main approach of the development is to create a medical product that a healthcare professional can use throughout a surgical intervention. From the viewpoint of product classification, the three main types of applications that are suitable to become TERM products to enhance regeneration are: pharmaceuticals, medical devices, and tissue products [1].

Among the three regulatory categories, the most abundant field of tissue engineering and the scope of the present investigation is scaffold development. The chosen development follows the tissue product pathway, which encompasses the utilization of decellularized bone, with the intended use to be applied in the musculoskeletal system [2].

Our approach within regenerative medicine aims to replace and repair lost or damaged tissues by stimulating the natural regeneration process [3]. Mesenchymal stem cells are multi-lineage cells, capable of self-renewal and differentiation into a variety of cell types [4], which play key roles in tissue healing and regenerative medicine. Bone-marrow-derived mesenchymal stem cells are the most frequently used stem cells in cell therapy and tissue engineering [5]. Allogeneic bone substitutes, such as fresh-frozen, freeze-dried, or demineralized bone, are commonly used in bone replacement interventions [6]. According to previous studies, freeze-dried human serum albumin is able to improve the adherence and proliferation of mesenchymal stem cells on bone allografts [7], and the serum albumin coating of the bone matrix showed stronger bone formation *in vivo* [8,9].

Lysophosphatidic acid (LPA) is a naturally occurring bioactive glycerophospholipid that is present in the systemic circulation in high nanomolar to low micromolar concentrations [10]. All LPA molecules consist of a glycerol backbone connected to a phosphate head group and ester-linked to an acyl chain [11]. The acyl chain length and degree of saturation of the formed LPA species are different. There are 16:0 > 18:0 > 20:4 > 18:1 > 18:2 LPAs that have been identified in resting and activated platelets. By contrast, in plasma, the rank order is 18:2 > 18:1  $\geq$  18:0 > 16:0 > 20:4, whereas in serum the order is 20:4 > 18:2 > 16:0  $\geq$  18:1 > 18:0 [12–14]. Extracellular LPA acts through at least six specific, G protein-coupled receptors (GPCRs), LPAR1-6, and regulates various cellular signaling pathways. LPA has a crucial role in numerous biological responses, including cell adhesion, migration, proliferation [15], differentiation [16], vascular development, wound healing, apoptosis regulation, and immunity [17,18].

In common with long-chain fatty acids, LPA binds with a high affinity to serum albumin, the main extracellular LPA binding protein, at a molar ratio of approximately 3:1 [19,20]. LPA binds to the primary high-affinity fatty acid-binding sites on albumin [19]. Albumin is necessary for the biological activity of LPA, and albumin concentration is critical for the activation of LPA receptors in a receptor-type-specific manner [21].

Under physiological conditions, osteoblast-produced LPA is present in bone tissue, and under some pathophysiological conditions, such as fracture healing, bone cells are exposed to high levels of platelet-derived LPA [22]. In different bone cells, LPA induces various cellular effects, including proliferation, differentiation, survival, and migration [23]. Furthermore, LPA contributes to angiogenesis which is also a key step during the bone regeneration process [24]. Due to these effects, LPA is a promising candidate for applications in bone regeneration [25]. In recent years, some biomaterial studies have supported the potential of LPA for use in bone tissue engineering applications. Mansell et al. found that albumin-bound LPA and calcitriol co-operate to promote osteoblast maturation on titanium and hydroxyapatite-coated surfaces [26] and improve human osteoblastogenesis [16]. A study reported by Bosetti et al. indicates that LPA and 1 $\alpha$ ,25-dihydroxy vitamin D<sub>3</sub>-enriched injectable scaffold can fasten bone fragments, leading to their apposition and new bone formation [27]. Furthermore, Binder et al. showed that physically entrapped LPA containing alginate hydrogel enhanced human bone marrow mesenchymal stem cell survival *in vivo* [28].

The very first criterion of any scaffold for tissue engineering is that it must be biocompatible [29]. Therefore, the present study aimed to investigate the biocompatibility of LPA and to determine the effect of the most abundant, albumin-bound 16:0, 18:1, and 18:2 LPA species on the proliferation and migration of human bone-marrow-derived mesenchymal stem cells.

## 2. Materials and Methods

### 2.1. Cell Culture and Materials

Human bone-marrow-derived mesenchymal stem cells (hBM-dMSCs) were purchased from ATCC (Manassas, VA, USA). The hBM-dMSCs were seeded in T75 TC-treated culture flasks and maintained at 37 °C in a 5% CO<sub>2</sub>, 95% humidified air incubator in the following stem cell medium: Dulbecco's modified Eagle's medium (DMEM) containing 4.5 g/L glucose and L-glutamine (Sigma-Aldrich, St. Louis, MO, USA) supplemented

with 10% fetal bovine serum (FBS; EuroClone, Pero, Italy), 1% Penicillin–streptomycin (Sigma-Aldrich, St. Louis, MO, USA), and 0.75 ng/mL basic fibroblast growth factor (Sigma-Aldrich, St. Louis, MO, USA). The culture medium was replaced three times a week. Cells with five to eight passages were used in the present study. In addition, 18:1 (oleoyl) and 18:2 (linoleoyl) LPA were purchased from Echelon Biosciences (Salt Lake City, UT, USA), and 16:0 (palmitoyl) LPA was purchased from Avanti Polar Lipids (Alabaster, AL, USA). For stock solutions, the lipids were dissolved in methanol, dried under nitrogen gas, and reconstituted in water immediately before use.

### 2.2. Fourier-Transform Infrared (FTIR) Spectroscopy

FTIR spectra of HSA-bound LPA species were compared with native HSA. Infrared measurements were performed with a Bruker Vertex 80v (Bruker Corp., Billerica, MA, USA) spectrometer, equipped with a high-sensitivity mercury–cadmium–telluride detector and a single reflection diamond ATR accessory. We collected 128 scans at a  $2\text{ cm}^{-1}$  resolution at the spectra wavelength range of  $4000\text{--}400\text{ cm}^{-1}$ . Further, 18:1, 18:2, or 16:0 LPA stock solutions of 1 mM concentration were mounted and surface-dried. A complex formation was initiated by mixing HSA and LPA with a peptide-to-lipid ratio of  $\sim 1:3$  using concentrations of  $300\text{ }\mu\text{M}$  and 1 mM for the HSA and the lipid, respectively. HSA- and LPA-containing solutions were mixed immediately before use.

### 2.3. Assessment of Cell Proliferation

The hBM-dMSCs were seeded on 96-well plates at 10,000 cells/well in  $200\text{ }\mu\text{L}$  stem cell medium and allowed to attach for 24 h. After attachment, the stem cell medium was changed to serum-free medium with or without 4% (*w/v*) fatty-acid-free human serum albumin (HSA, Seracare, Milford, MA, USA) and the cells were cultured in the new medium overnight. Then the cells were treated with either 18:1, 18:2 or 16:0 LPA ( $0.1\text{--}0.3\text{--}1\text{--}3\text{--}10\text{ }\mu\text{M}$ ) for 24 h. After treatment, the cell proliferation was measured using Cell Proliferation Kit II (XTT; Roche, Mannheim, Germany), according to the manufacturer's instructions. Cell proliferation is expressed as a percentage of the data of the HSA or native control group.

### 2.4. Wound Healing Assay

The hBM-dMSCs were allowed to grow on 24-well plates in  $500\text{ }\mu\text{L}$  stem cell medium until they reached a confluent monolayer. The stem cell medium was changed to serum-free medium with or without 4% HSA, and the cells were incubated overnight. A cell-free zone was created across the cell monolayer with a sterile plastic micropipette tip in each well. After washing with Dulbecco's phosphate-buffered saline (PBS; Sigma-Aldrich, St. Louis, MO, USA), the cells were treated with 18:1, 18:2, or 16:0 LPA ( $1\text{--}3\text{--}10\text{ }\mu\text{M}$ ) alone or in combination with HSA. Cell migration was examined for 24 h with live cell imaging using a Nikon Eclipse Ti2 microscope (Nikon Corporation, Tokyo, Japan). The images were analyzed after 0, 12, and 24 h of treatment, and the wound area was calculated by tracing the cell-free area in captured images using Nikon NIS-Elements Analysis Software (v.5.19, Nikon Corporation, Tokyo, Japan). The migration rate is expressed as the percentage of area reduction.

### 2.5. Statistical Analysis

All data are presented as mean  $\pm$  SEM. The normal distribution of datasets was verified with the Kolmogorov–Smirnov test. If the normal distribution was confirmed, data are presented as the arithmetic mean and standard error, and the *p*-values were determined by a two-way ANOVA followed by Tukey's multiple comparison test. If data are not normally distributed, data are presented as the median and interquartile range, and the statistical significance was determined by a Kruskal–Wallis test followed by Dunn's multiple comparisons. Statistical analysis and graph plotting were performed using GraphPad Prism software (v.6.0; GraphPad Software Inc., La Jolla, CA, USA), and  $p < 0.05$  was considered a statistically significant difference.

### 3. Results

#### 3.1. Assessment of Albumin–LPA Complex Formation with FTIR

The FTIR measurement results are shown in Figure 1, where structure-related chemical changes are demonstrated. The absorbances were normalized to the  $2916\text{ cm}^{-1}$  peak in the case of LPA species, and the spectra were vertically shifted for a better understanding and to prevent overlapping. Figure 1A shows the FTIR spectra of native 18:2, 18:1, and 16:0 LPA species, whereas the spectra of HSA and HSA-bound 18:2, 18:1, and 16:0 LPA are shown in Figure 1B. These absorbances were normalized to the absorbance peak at  $1648\text{ cm}^{-1}$ .

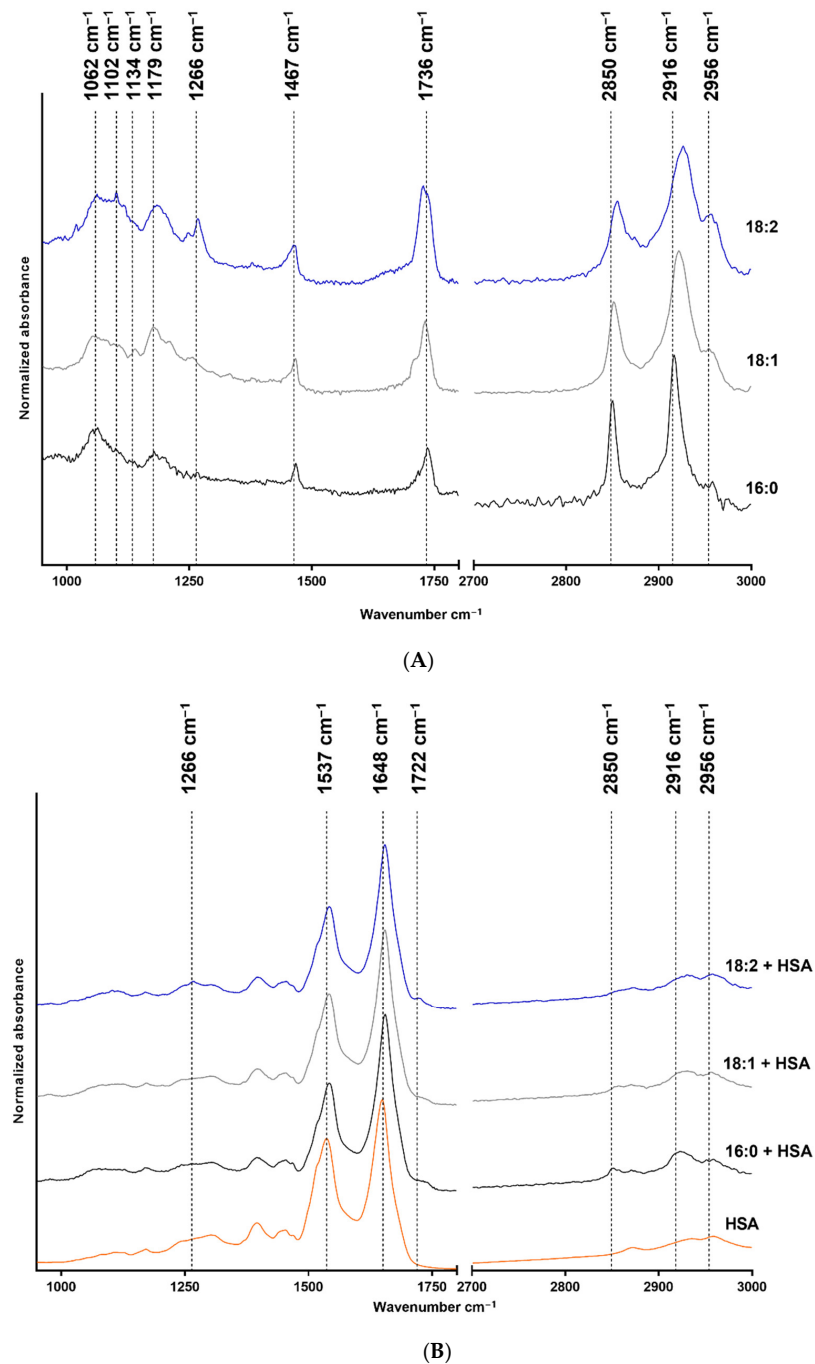


**Figure 1.** FTIR spectra of native and HSA-bound LPA species and native HSA. (A) Native 16:0 LPA is shown at the bottom, 18:1 in the middle, and 18:2 at the top of the image. (B) The bottom line shows the FTIR spectra of native HSA and, in a vertical sequence, HSA-bound 16:0, 18:1, and 18:2 LPA species are shown.

In the case of the FTIR spectra of LPA species, the main absorbances were characteristic for the CH<sub>2</sub> groups, the C=O groups, C-O bonds, and P-O-C bonds. In the case of HSA, the two characteristic bonds were the amide I and amide II absorption bands.

### 3.2. Effects of LPA Species on hBM-dMSCs Proliferation

XTT measurements were performed to investigate the possible cytotoxicity and to evaluate the effects of 18:1, 18:2, and 16:0 LPA on the proliferation of hBM-dMSCs. The cells were treated with increasing concentrations of phospholipids alone or in combination with HSA. After 24 h of treatment, none of the three LPA species showed cytotoxic effects up to 10  $\mu$ M concentration. 18:1 LPA in 1, 3, and 10  $\mu$ M concentrations significantly increased cell proliferation compared with the control group, but solely when administered in the presence of HSA (Figure 2A). In addition, 18:2 LPA significantly enhanced the proliferation of hBM-dMSCs in combination with HSA in 1, 3, and 10  $\mu$ M and when examined alone in 3 and 10  $\mu$ M concentrations (Figure 2B). A significant elevation in the cell proliferation was caused by 0.3, 1, 3, and 10  $\mu$ M 16:0 LPA treatment, exclusively in combination with HSA (Figure 2C). Interestingly, among the examined three LPA species, only 18:2 LPA in 3 and 10  $\mu$ M concentrations significantly increased cell proliferation when administered without HSA (Figure 2B).

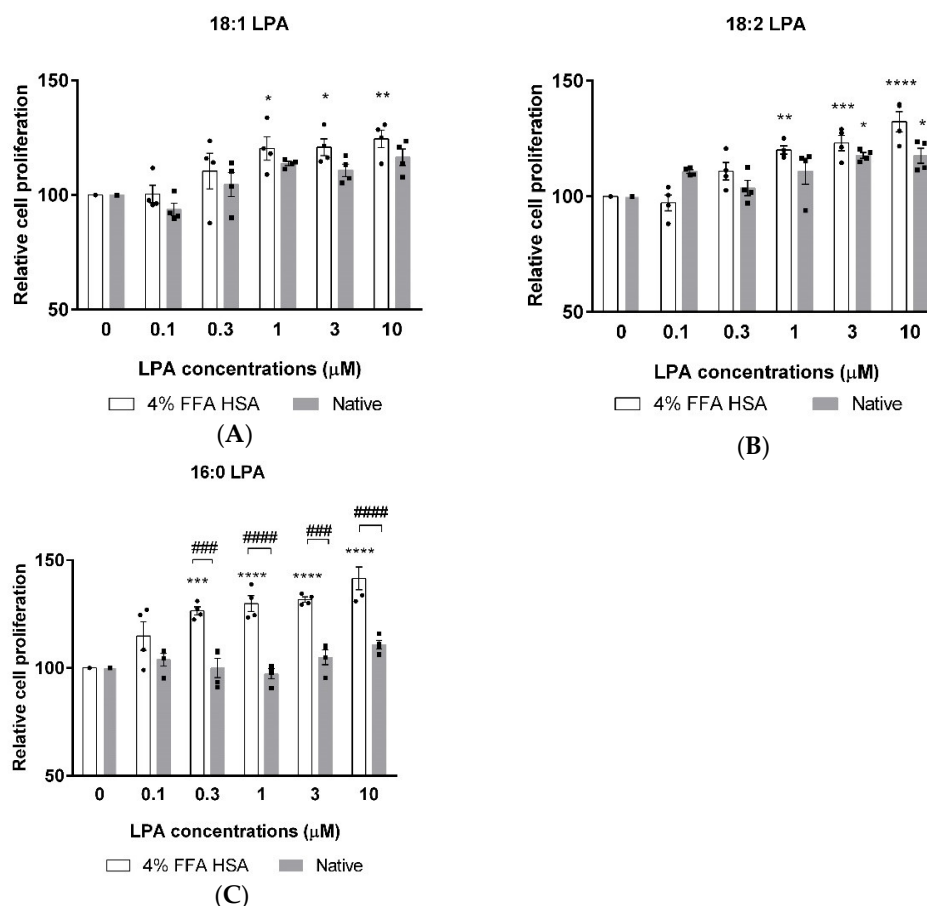


**Figure 2.** Relative cell proliferation after 18:1 (A), 18:2 (B) and 16:0 (C) LPA treatment in combination with HSA (4% FFA HSA, white columns) or alone (native, grey columns). (\*  $p < 0.05$ , \*\*  $p < 0.01$ , \*\*\*  $p < 0.001$ , \*\*\*\*  $p < 0.0001$  vs. control (0  $\mu$ M LPA), ###  $p < 0.001$ , ####  $p < 0.0001$ ,  $n = 4$  in each group, two-way ANOVA, followed by Tukey's multiple comparison test). Data are presented as % of control and mean  $\pm$  SEM.

### 3.3. The Effect of LPA Species on the Migration of hBM-dMSCs

Thereafter, we investigated whether 18:1, 18:2, or 16:0 LPA influenced the migration of the hBM-dMSCs, in a wound healing assay (Figure 3). The initial scratch area did not

differ significantly in the treatment groups. The cells did not completely fill the gaps after 24 h of treatment. However, none of the three LPA species significantly enhanced cell migration, neither 12 nor 24 h after treatment, compared with the control group. There was also no significant difference between the HSA-bound LPA and the native LPA-treated groups (Figure 4). HSA-bound 16:0 LPA in a 10  $\mu$ M concentration significantly improved the migration of the cells after 12 h, compared with a 1  $\mu$ M concentration, the effect of which was not observable after 48 h of treatment (Figure 4C).

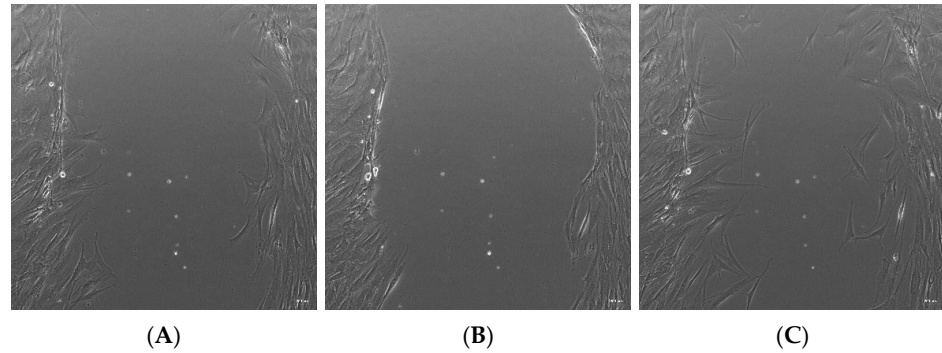


**Figure 3.** Representative bright-field images of the in vitro wound healing assay. (A) The “wound” was created by a line scratch across the hBM-dMSCs monolayer. Images were analyzed after (B) 12 and (C) 24 h of treatment. The images were taken in 10 $\times$  magnification, and the scale bar represents 200  $\mu$ m.

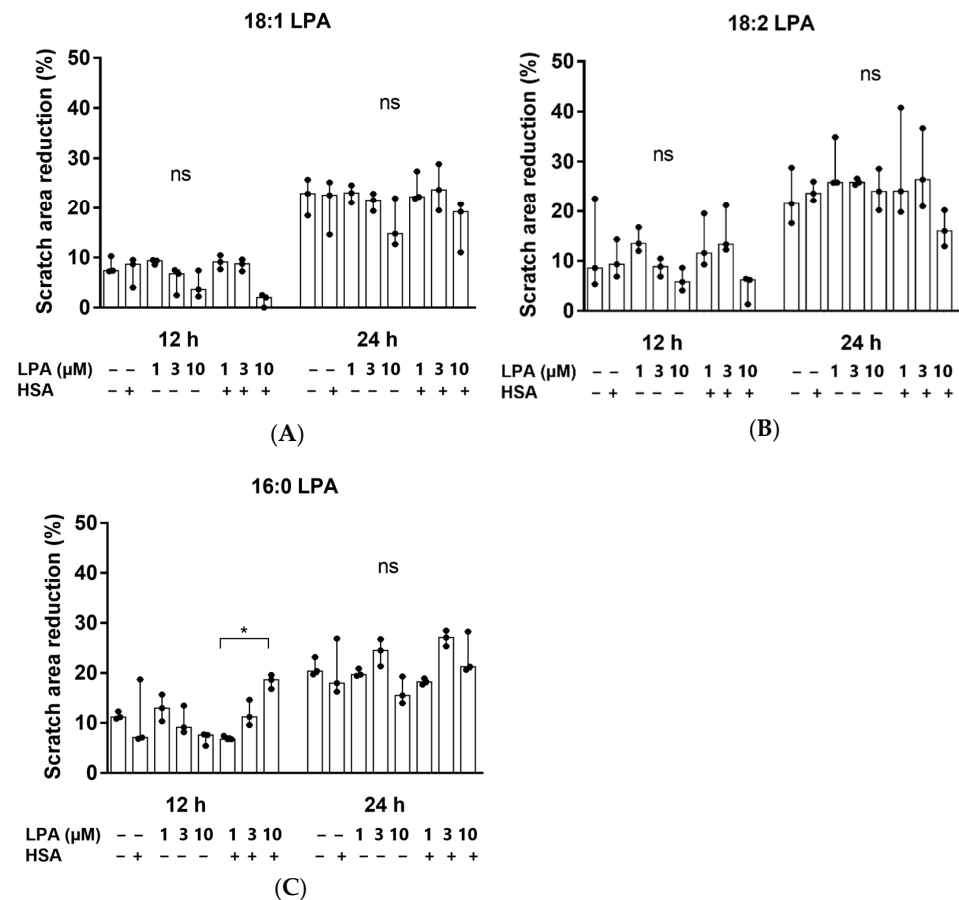


**Figure 4.** Scratch area reduction (%) after treatment with (A) 18:1, (B) 18:2 and (C) 16:0 LPA species for 12 and 24 h. hBM-dMSCs were treated with different LPA species in 1  $\mu$ M, 3  $\mu$ M, and 10  $\mu$ M concentrations alone or in combination with HSA (\*  $p < 0.05$ ,  $n = 3$ , Kruskal–Wallis test followed by Dunn’s multiple comparison test). Data are presented as the median and interquartile range. The migration rate is expressed as the percentage of area reduction.

#### 4. Discussion

The IR spectra were assessed for all three LPA derivatives. To enable this, only the characteristic functional groups were measured, and no interference occurred. Fatty acid-free HSA was used; thus it did not contain any complex-forming molecules. The LPA was solubilized in methanol and water to avoid any secondary binding and to ensure the purity of the reagents for spectroscopic purposes. The stretching of the CH<sub>2</sub> groups is visible in the 2916–2926 cm<sup>-1</sup> range and around 2850 cm<sup>-1</sup>. The deformation vibrations occur at 1467 cm<sup>-1</sup> [30], and at 1736 cm<sup>-1</sup> C=O stretching is visible [31]. The absorbance at 1266 cm<sup>-1</sup> has been described as the peak of the PO<sub>2</sub> asymmetric stretching vibration. However, this absorption is more profound in the spectrum of 18:2 LPA but should also appear in the spectra of 18:1 and 16:0 derivatives. Alternatively, this band can result from the CH<sub>α</sub> rocking, which is visible in the case of double bonds, and which is likely to be more intense in the case of 18:2 LPA, due to the two double bonds [32]. The purity of LPA 18:1 and 18:2 is in the 90 % range; thus, it may also be an acyl isomer impurity. The P-O-C and C-O bonds appear at 1062 cm<sup>-1</sup> and 1179 cm<sup>-1</sup>, respectively [33]. Both CH<sub>2</sub> stretching absorbances shifted towards higher wavenumbers in the case of LPA derivatives, with an 18-carbon-atom acyl chain length compared with the 16-carbon-atom acyl chain length LPA. The increased CH<sub>2</sub> stretching frequencies indicate the higher disorder of the chains caused by the presence of double bonds in the acyl chains. The LPA derivatives are known to form complexes with HSA [19] in the 1:3 HSA:LPA ratio. Thus, the formed complexes were measured with the use of FTIR to investigate whether absorbance shifting occurred. HSA peaks dominate in the spectrum compared with the LPA peaks, which is presumably due to the significant difference in the molecular weights of the components. The two main characteristic bands for albumin are the amide I and II bands at 1648 cm<sup>-1</sup>, and at 1537 cm<sup>-1</sup>, respectively [34,35]. According to our evaluation, there was a small spectral shift of the amide I band in presence of LPA. The spectral shift was 1 cm<sup>-1</sup> in the case of bound 18:1 LPA, and 3 cm<sup>-1</sup> in the case of 18:2 and 16:0 LPA variants. These variations indicate a subtle change in the secondary structure, while preserving the overall alpha-helical nature of the protein. A similar shift was observed in the case of the amide II band. These spectral changes in the amide bands might indicate the binding of LPA to HSA.

Earlier, Chen et al. showed that LPA protects hBM-dMSCs against hypoxia and serum deprivation-induced apoptosis *in vitro*, indicating that LPA is a potent survival factor for hBM-dMSCs in bone repair applications [36]. In addition, LPA was observed to promote H<sub>2</sub>O<sub>2</sub>-induced autophagy [37], the effect of which was shown to play important roles in cell survival [38]. These findings make LPA a promising candidate to improve the viability and proliferation of hBM-MSCs during bone healing. Our cell viability measurement data demonstrate that 18:1, 18:2 and 16:0 LPA species are non-toxic for hBM-dMSCs up to 10 μM concentration. Although there is evidence for the advantages of using LPA in bone regenerative medicine [26,27], there are still some challenges with the *in vivo* application of LPA. LPA is easily degraded *in vivo* by lipid phosphate phosphatases [39]; thus, LPA requires a carrier that allows the successful delivery of the lipid. In our experiments, all the three tested LPA species improved the proliferation of hBM-dMSCs, the effect of which was more pronounced when administered in the presence of HSA. This finding supports the assumption that HSA might serve as an ideal carrier for LPA in bone regenerative applications. Further, 18:1 and 16:0 LPA species did not significantly improve the cell proliferation without HSA. However, interestingly, this effect appeared in the case of 18:2 LPA in 3 and 10 μM concentrations. The regulated signaling pathway during this LPA effect is not yet evaluated. However it is possible that these LPA species need to be transported to their receptors for signaling pathway activation. The proliferative effect of LPA seemed to be dose-dependent. The highest increments in cell proliferation were shown in 18:2 LPA in 3 and 10 μM and 16:0 LPA in 0.3, 1, 3, and 10 μM concentrations.

LPA is known to mediate the migration of various cell types [40,41], which might be connection to the experienced, LPA-enhanced proliferation of the hBM-dMSCs. In a previous research article by Song et al., LPA induced the migration of hBM-dMSCs [42].

Thus, as our next step, we investigated whether LPA in the presence or absence of HSA affects the migration of hBM-dMSCs. However, no significant increase was observed. Hence, it seems that, in our case, the viability-enhancing effect of LPA is not directly proportional to the migration in the case of hBM-dMSCs.

## 5. Conclusions

During our experiments, the main goal was to investigate the potential effect of LPA species on the viability of hBM-dMSCs, *in vitro*. The experiments included the toxicity profile of various concentrations of 18:1, 18:2 and 16:0 LPA species alone or in combination with HSA to investigate if the addition of LPA is beneficial for the attachment, proliferation, and migration of hBM-dMSCs. The complex formation between HSA and LPA was also analyzed with the use of IR spectroscopy. With these experiments, we aimed to find out if there is any difference in the spectra of the formed complexes compared with the base materials that could be visualized with IR spectroscopy. Thus, the characteristic peaks were compared in order to determine if any shifting of the absorbance wavelength of the characteristic peaks occurs. We found small spectral shifts of the amide I and II bands of HSA in the presence of LPA, indicating subtle changes in the secondary structure of the HSA due to the binding of LPA. The effect of LPA was also evaluated *in vitro*, with the use of XTT and migration assay in hBM-dMSCs. We found that LPA enhances the viability of hBM-dMSCs alone, the effect of which is more pronounced when administered in combination with HSA. In summary, in the present study, we have demonstrated that LPA is suitable for increasing cell viability alone and in combination with HSA *in vitro*, which may be a useful supplementation in TERM-related applications.

**Author Contributions:** Conceptualization, A.M., I.H. and É.R.; methodology, A.M., I.H., J.P., A.H. and B.B.; investigation, A.M., I.H., J.P. and L.S.; data curation, A.M. and I.H.; writing—original draft preparation, A.M.; writing—review and editing, I.H., É.R.; visualization, A.M. and I.H.; supervision, I.H. and É.R.; funding acquisition, Z.B. and Z.L. All authors have read and agreed to the published version of the manuscript.

**Funding:** Prepared with the professional support of the Doctoral Student Scholarship Program of the Co-operative Doctoral Program of the Ministry of Innovation and Technology financed from the National Research, Development and Innovation Fund, KDP-2020. This research was also funded by the Hungarian National Research, Development and Innovation Office, TKP2021-EGA-25, TKP2021-EGA-21, 2020-1.1.6-JÖVŐ-2021-00010, 2020-1.1.6-JÖVŐ-2021-00013, OTKA K-125174, PD-132851, K-135683, and K-139230 grants and by the Higher Education Institutional Excellence Program of the Ministry of Human Capacities in Hungary, within the framework of the Molecular Biology thematic program of the Semmelweis University, with support from the EFOP-3.6.3-VEKOP-16-2017-00009 grant. The Central Library of Semmelweis University also kindly provided funds for open access publication fees.

**Institutional Review Board Statement:** The study was conducted according to the guidelines of the Declaration of Helsinki and approved by the Institutional Review Board of EÜIG (29152-3/2019).

**Informed Consent Statement:** Informed consent was obtained from all subjects involved in the study.

**Data Availability Statement:** The data presented in this study are available on request from the corresponding author.

**Acknowledgments:** The authors are thankful to OrthoSera Medical Zrt., and the Department of Materials Science and Technology, University of Győr for the research support.

**Conflicts of Interest:** The authors declare no conflict of interest.

## References

1. Frey, B.M.; Zeisberger, S.M.; Hoerstrup, S.P. Tissue Engineering and Regenerative Medicine-New Initiatives for Individual Treatment Offers. *Transfus. Med. Hemother.* **2016**, *43*, 318–320. [[CrossRef](#)] [[PubMed](#)]
2. Hinsenkamp, A.; Benyó, Z.; Hornyák, I. Overview of Tissue Engineering Patent Strategies and Patents from 2010 to 2020, Including Outcomes. *Tissue Eng. Part B Rev.* **2022**, *28*, 626–632. [[CrossRef](#)] [[PubMed](#)]
3. Gardner, R.L. Stem cells and regenerative medicine: Principles, prospects and problems. *C. R. Biol.* **2007**, *330*, 465–473. [[CrossRef](#)] [[PubMed](#)]
4. Bianco, P.; Robey, P.G.; Simmons, P.J. Mesenchymal stem cells: Revisiting history, concepts, and assays. *Cell Stem. Cell* **2008**, *2*, 313–319. [[CrossRef](#)]
5. Fu, X.; Liu, G.; Halim, A.; Ju, Y.; Luo, Q.; Song, A.G. Mesenchymal Stem Cell Migration and Tissue Repair. *Cells* **2019**, *8*, 784. [[CrossRef](#)]
6. Holzmann, P.; Niculescu-Morzsza, E.; Zwickl, H.; Halbwirth, F.; Pichler, M.; Matzner, M.; Gottsauner-Wolf, F.; Nehrer, S. Investigation of bone allografts representing different steps of the bone bank procedure using the CAM-model. *Altex* **2010**, *27*, 97–103. [[CrossRef](#)]
7. Weszl, M.; Skaliczki, G.; Cselenyák, A.; Kiss, L.; Major, T.; Schandl, K.; Bognár, E.; Stadler, G.; Peterbauer, A.; Csöngé, L.; et al. Freeze-dried human serum albumin improves the adherence and proliferation of mesenchymal stem cells on mineralized human bone allografts. *J. Orthop. Res.* **2012**, *30*, 489–496. [[CrossRef](#)]
8. Horváthy, D.B.; Vác, G.; Szabó, T.; Szigyártó, I.C.; Toró, I.; Vámos, B.; Hornyák, I.; Renner, K.; Klára, T.; Szabó, B.T.; et al. Serum albumin coating of demineralized bone matrix results in stronger new bone formation. *J. Biomed. Mater. Res. B Appl. Biomater.* **2016**, *104*, 126–132. [[CrossRef](#)]
9. Horváthy, D.B.; Schandl, K.; Schwarz, C.M.; Renner, K.; Hornyák, I.; Szabó, B.T.; Niculescu-Morzsza, E.; Nehrer, S.; Dobó-Nagy, C.; Doros, A.; et al. Serum albumin-coated bone allograft (BoneAlbumin) results in faster bone formation and mechanically stronger bone in aging rats. *J. Tissue Eng. Regen. Med.* **2019**, *13*, 416–422. [[CrossRef](#)]
10. Moolenaar, W.H. Lysophosphatidic acid, a multifunctional phospholipid messenger. *J. Biol. Chem.* **1995**, *270*, 12949–12952. [[CrossRef](#)]
11. Yung, Y.C.; Stoddard, N.C.; Chun, J. LPA receptor signaling: Pharmacology, physiology, and pathophysiology. *J. Lipid Res.* **2014**, *55*, 1192–1214. [[CrossRef](#)] [[PubMed](#)]
12. Aoki, J. Mechanisms of lysophosphatidic acid production. *Semin. Cell Dev. Biol.* **2004**, *15*, 477–489. [[CrossRef](#)]
13. Aikawa, S.; Hashimoto, T.; Kano, K.; Aoki, J. Lysophosphatidic acid as a lipid mediator with multiple biological actions. *J. Biochem.* **2015**, *157*, 81–89. [[CrossRef](#)] [[PubMed](#)]
14. Sano, T.; Baker, D.; Virag, T.; Wada, A.; Yatomi, Y.; Kobayashi, T.; Igarashi, Y.; Tigyi, G. Multiple mechanisms linked to platelet activation result in lysophosphatidic acid and sphingosine 1-phosphate generation in blood. *J. Biol. Chem.* **2002**, *277*, 21197–21206. [[CrossRef](#)] [[PubMed](#)]
15. Liu, Y.B.; Kharode, Y.; Bodine, P.V.; Yaworsky, P.J.; Robinson, J.A.; Billiard, J. LPA induces osteoblast differentiation through interplay of two receptors: LPA1 and LPA4. *J. Cell. Biochem.* **2010**, *109*, 794–800. [[CrossRef](#)]
16. Mansell, J.P.; Nowghani, M.; Pabbruwe, M.; Paterson, I.C.; Smith, A.J.; Blom, A.W. Lysophosphatidic acid and calcitriol co-operate to promote human osteoblastogenesis: Requirement of albumin-bound LPA. *Prostaglandins Other Lipid Mediat.* **2011**, *95*, 45–52. [[CrossRef](#)]
17. Li, Y.F.; Li, R.S.; Samuel, S.B.; Cueto, R.; Li, X.Y.; Wang, H.; Yang, X.F. Lysophospholipids and their G protein-coupled receptors in atherosclerosis. *Front. Biosci.* **2016**, *21*, 70–88. [[CrossRef](#)]
18. Chen, C.; Ochoa, L.N.; Kagan, A.; Chai, H.; Liang, Z.; Lin, P.H.; Yao, Q. Lysophosphatidic acid causes endothelial dysfunction in porcine coronary arteries and human coronary artery endothelial cells. *Atherosclerosis* **2012**, *222*, 74–83. [[CrossRef](#)]
19. Thumser, A.E.; Voysey, J.E.; Wilton, D.C. The binding of lysophospholipids to rat liver fatty acid-binding protein and albumin. *Biochem. J.* **1994**, *301 Pt 3*, 801–806. [[CrossRef](#)]
20. Michalczyk, A.; Budkowska, M.; Dołęgowska, B.; Chlubek, D.; Safranow, K. Lysophosphatidic acid plasma concentrations in healthy subjects: Circadian rhythm and associations with demographic, anthropometric and biochemical parameters. *Lipids Health Dis.* **2017**, *16*, 140. [[CrossRef](#)]
21. Hama, K.; Bando, K.; Kakehi, Y.; Aoki, J.; Arai, H. Lysophosphatidic acid (LPA) receptors are activated differentially by biological fluids: Possible role of LPA-binding proteins in activation of LPA receptors. *FEBS Lett.* **2002**, *523*, 187–192. [[CrossRef](#)]
22. Karagiosis, S.A.; Karin, N.J. Lysophosphatidic acid induces osteocyte dendrite outgrowth. *Biochem. Biophys. Res. Commun.* **2007**, *357*, 194–199. [[CrossRef](#)] [[PubMed](#)]
23. Yu, Z.L.; Jiao, B.F.; Li, Z.B. Lysophosphatidic Acid Analogue rather than Lysophosphatidic Acid Promoted the Bone Formation In Vivo. *Biomed. Res. Int.* **2018**, *2018*, 7537630. [[CrossRef](#)] [[PubMed](#)]
24. Chen, Y.; Ramakrishnan, D.P.; Ren, B. Regulation of angiogenesis by phospholipid lysophosphatidic acid. *Front. Biosci.* **2013**, *18*, 852–861. [[CrossRef](#)]
25. Wu, X.; Ma, Y.; Su, N.; Shen, J.; Zhang, H.; Wang, H. Lysophosphatidic acid: Its role in bone cell biology and potential for use in bone regeneration. *Prostaglandins Other Lipid Mediat.* **2019**, *143*, 106335. [[CrossRef](#)]

26. Mansell, J.P.; Barbour, M.; Moore, C.; Nowghani, M.; Pabbruwe, M.; Sjostrom, T.; Blom, A.W. The synergistic effects of lysophosphatidic acid receptor agonists and calcitriol on MG63 osteoblast maturation at titanium and hydroxyapatite surfaces. *Biomaterials* **2010**, *31*, 199–206. [[CrossRef](#)]
27. Bosetti, M.; Borrone, A.; Leigheb, M.; Shastri, V.P.; Cannas, M. (\*) Injectable Graft Substitute Active on Bone Tissue Regeneration. *Tissue Eng. Part A* **2017**, *23*, 1413–1422. [[CrossRef](#)]
28. Binder, B.Y.; Williams, P.A.; Silva, E.A.; Leach, J.K. Lysophosphatidic Acid and Sphingosine-1-Phosphate: A Concise Review of Biological Function and Applications for Tissue Engineering. *Tissue Eng. Part B Rev.* **2015**, *21*, 531–542. [[CrossRef](#)]
29. O'Brien, F.J. Biomaterials & scaffolds for tissue engineering. *Mater. Today* **2011**, *14*, 88–95. [[CrossRef](#)]
30. Estrela-Lopis, I.; Brezesinski, G.; Möhwald, H. Dipalmitoyl-phosphatidylcholine/phospholipase D interactions investigated with polarization-modulated infrared reflection absorption spectroscopy. *Biophys. J.* **2001**, *80*, 749–754. [[CrossRef](#)]
31. Villé, H.; Maes, G.; De Schrijver, R.; Spincemaille, G.; Rombouts, G.; Geers, R. Determination of phospholipid content of intramuscular fat by Fourier Transform Infrared spectroscopy. *Meat Sci.* **1995**, *41*, 283–291. [[CrossRef](#)]
32. Movasaghi, Z.; Rehman, S.; ur Rehman, D.I. Fourier Transform Infrared (FTIR) Spectroscopy of Biological Tissues. *Appl. Spectrosc. Rev.* **2008**, *43*, 134–179. [[CrossRef](#)]
33. Nzai, J.M.; Proctor, A. Determination of phospholipids in vegetable oil by fourier transform infrared spectroscopy. *J. Am. Oil Chem. Soc.* **1998**, *75*, 1281–1289. [[CrossRef](#)]
34. Alhazmi, H.A. FT-IR Spectroscopy for the Identification of Binding Sites and Measurements of the Binding Interactions of Important Metal Ions with Bovine Serum Albumin. *Sci. Pharm.* **2019**, *87*, 5. [[CrossRef](#)]
35. Hinsenkamp, A.; Ézsiás, B.; Pál, É.; Hricisák, L.; Fülöp, Á.; Besztercei, B.; Somkuti, J.; Smeller, L.; Pinke, B.; Kardos, D.; et al. Crosslinked Hyaluronic Acid Gels with Blood-Derived Protein Components for Soft Tissue Regeneration. *Tissue Eng. Part A* **2021**, *27*, 806–820. [[CrossRef](#)] [[PubMed](#)]
36. Chen, J.; Baydoun, A.R.; Xu, R.; Deng, L.; Liu, X.; Zhu, W.; Shi, L.; Cong, X.; Hu, S.; Chen, X. Lysophosphatidic acid protects mesenchymal stem cells against hypoxia and serum deprivation-induced apoptosis. *Stem Cells* **2008**, *26*, 135–145. [[CrossRef](#)]
37. Wang, X.-Y.; Fan, X.-S.; Cai, L.; Liu, S.; Cong, X.-F.; Chen, X. Lysophosphatidic acid rescues bone mesenchymal stem cells from hydrogen peroxide-induced apoptosis. *Apoptosis* **2015**, *20*, 273–284. [[CrossRef](#)]
38. Baehrecke, E.H. Autophagy: Dual roles in life and death? *Nat. Rev. Mol. Cell Biol.* **2005**, *6*, 505–510. [[CrossRef](#)]
39. Salous, A.K.; Panchatcharam, M.; Sunkara, M.; Mueller, P.; Dong, A.; Wang, Y.; Graf, G.A.; Smyth, S.S.; Morris, A.J. Mechanism of rapid elimination of lysophosphatidic acid and related lipids from the circulation of mice. *J. Lipid Res.* **2013**, *54*, 2775–2784. [[CrossRef](#)]
40. Jans, R.; Mottram, L.; Johnson, D.L.; Brown, A.M.; Sikkink, S.; Ross, K.; Reynolds, N.J. Lysophosphatidic acid promotes cell migration through STIM1- and Orai1-mediated Ca<sup>2+</sup>(i) mobilization and NFAT2 activation. *J. Investig. Dermatol.* **2013**, *133*, 793–802. [[CrossRef](#)]
41. Kim, E.K.; Yun, S.J.; Do, K.H.; Kim, M.S.; Cho, M.; Suh, D.-S.; Kim, C.D.; Kim, J.H.; Birnbaum, M.J.; Bae, S.S. Lysophosphatidic acid induces cell migration through the selective activation of Akt1. *Exp. Mol. Med.* **2008**, *40*, 445–452. [[CrossRef](#)] [[PubMed](#)]
42. Song, H.Y.; Lee, M.J.; Kim, M.Y.; Kim, K.H.; Lee, I.H.; Shin, S.H.; Lee, J.S.; Kim, J.H. Lysophosphatidic acid mediates migration of human mesenchymal stem cells stimulated by synovial fluid of patients with rheumatoid arthritis. *Biochim. Biophys. Acta* **2010**, *1801*, 23–30. [[CrossRef](#)] [[PubMed](#)]